Winding virtual rolls

B.K. KANDADAI AND J.K. GOOD

ABSTRACT: The winding of web materials is a subject of economic import that has resulted in mechanics analysis and model development. Many materials are wound into rolls for storage and subsequent processing. Winding is an accretive process in which the internal stresses within each layer of the wound roll are affected by the web layers that have been most recently added. As rolls wind, the edges take the approximate shape of an Archimedean spiral. All analyses and models to date have imposed the assumption that this spiral form can be replaced by a series of concentric web layers that are added one by one to the exterior of the model of the winding roll. It was also assumed that the bending stresses and strains associated with winding a flat web into a wound roll are negligible, an assumption with a validity that is highly dependent on web thickness.

In this investigation, the web will be attached to a core and wound in a spiral form from the start to the completion of the wound roll. It will be shown that modeling the spiral geometry of the web in a wound roll can be beneficial in understanding stress concentrations in the vicinity of the starting position of the web on the core and for understanding how nip rollers can affect the web tension in the outer layer of a winding roll.

Application: This research shows how explicit finite element modeling can be used to wind rolls of web materials. It also shows how this type of modeling can be used to solve winding problems that cannot be solved by other methods.

Many consumer and industrial products are produced from paper, plastic film, and nonwoven webs with widths that greatly exceed their thicknesses and lengths that greatly exceed their widths. Webs are stored in the form of rolls that may be unwound, processed and rewound many times before the web is converted to a final product. Though the winding is necessary, it is frequently responsible for losses in product quality and therefore, profits, so it must be done carefully.

Many references are found in the literature where winding of webs is investigated. The result of these investigations was often winding models that relate winder operating parameters and web and core material parameters to output parameters such as internal pressure and web stresses. If roll defects could be quantified in terms of these outputs, then they could be avoided by seeking winder operating parameters that would limit the pressure or stress that was responsible for the defect. Theoretical investigations of winding and wound roll models can broadly be classified into the following categories based on the solution approach:

- Closed form solutions based on linear elastic theory.
- Numerical solutions based on linear elastic, viscoelastic, thermoelastic, large deformation continuum, or energy formulations.
- Numerical solutions based on accretive axisymmetric finite element (FE) formulations.
- Numerical solutions with the use of commercial FE codes.

Many of the analytical and numerical models classified above have been reviewed by Good and Roisum [1]. Only a few authors have focused on the analysis of wound rolls using FE methods. These investigations focused on the impact of web thickness and length variation on wound roll shape and stresses [2,3]. Commercial FE codes have primarily been used to study the effect of roll weight, gravity, etc., on the wound roll structure. Some of the examples include the coil collapse FE simulations of Smolinski et al. [4] and Li and Cao [5]. Arola and von Hertzen [6] analyzed the development of sheet tension under a rolling nip on a paper stack using explicit FE methods. Recently, in another study [7], Arola and von Hertzen used an elastoplastic continuum model in an explicit formulation to study the slippage within the wound roll. The same model was extended to study the effect of clamping forces on the deformation of the wound rolls. Be it a classical or a numerical approach, all the authors have assumed that the wound roll is a set of concentric hoops and that the bending strains and stresses associated with making the flat web conform to a wound roll are negligible.

At the beginning of a winding operation, the web will be attached to the winding core and the winder is started. For many webs, it is noted that there is a visible presence of a radial disturbance at the outside of the winding roll at the same circumferential location where the web was adhered to the core. Some webs have high radial compressibility, and this disturbance may be visible only while the first layers are added to the core. Other webs with low radial compressibility may still exhibit this radial disturbance after winding has been completed and thousands of web layers have been wound onto the core. When unwound, the web may have a permanent crease in the web across the web width in the cross direction (CD) that may or may not be acceptable and may repeat for every revolution of the unwinding roll.

Many webs are wound with a roller impinged at the outer radius of the winding roll that may be driven or undriven. The impinged roller may serve to limit the amount of air that is wound into the winding roll, but it also serves to modify the tension in the outer layer(s) by locally inducing slippage between web layers in the zone of contact between the impinged and winding rolls. This slippage cannot be directly modeled using the previously developed winding models. The slippage would result in relative circumferential motion between layers that is not defined for these models.

For the problems described previously, the spiral geometry of the wound roll is an important detail that must be modeled. Except for viscoelastic material effects, the winding models that assume the wound roll can be modeled as concentric hoops of material are decoupled from time. We will model the process of winding a flat web into a spiral geometry on a core using an explicit time dependent finite element formulation to explore the problems described.

Property	Value
Web length	509.5 cm
Web thickness (Caliper)	0.254 cm
Rigid core diameter	8.89 cm
Rigid nip roller diameter	10.16 cm
Final wound roll diameter	15.61 cm*
Angular velocity (ω_c)	0.5 rad/sec
Coefficient of friction ($\mu_{Nw}, \mu_{ww}, \mu_{cw}$)	0.2, 0.2, 0.2
Web tension (T_w)	2.6, 4.4, 6.1 N/cm
Nip load (N)	8.8, 17.5, 26.3, 35 N/cm
Web Young's modulus (E), Poisson's ratio (ν)	69 MPa, 0.3
Web density (ρ)	1.25 g/cm^3
*This value is approximate and will vary depending on winding conditions.	

I. Winding model properties.

WOUND ROLL FINITE ELEMENT MODEL

During the startup sequence of a winder, the incoming pretensioned layer is fastened to the core. The winder is started and layers are wound in a spiral fashion upon the core. In the models presented, it is assumed that the torque required to wind the rolls will be provided at the core (e.g., a center winder).

Model setup

The model is set up such that it resembles the real winding process closely. Consider an initial configuration in which the incoming web layer is tied to the rigid core, as **Fig. 1a** shows. The core and the nip roller (in the case of center winding with an undriven nip roller) are modeled as rigid cylindrical bodies. The web is modeled as an elastic layer of constant thickness. Winding is then accomplished in different steps that are a function of time in ABAQUS/Explicit (a commercial FE program from Dassault Systems Simulia; Providence, RI, USA).

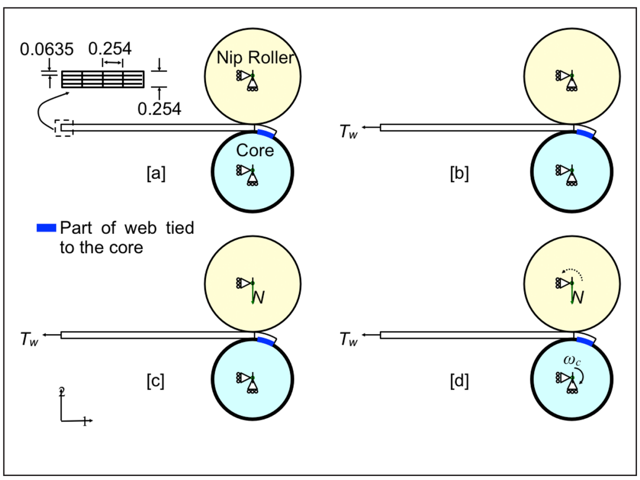

1. Schematic representation of the finite element (FE) model setup.

In the first time step, the web tension (the distributed load T_w) is prescribed at the left end of the sheet. A constant web tension will be simulated in the incoming sheet, as Fig. 1b shows. In this time step, the center of rotation of the core is fixed in all degrees of freedom, and the nip roller is pinned.

In the second time step, the nip roller contacts the incoming web under a prescribed nip load (N). In this time step, the boundary conditions are modified such that the center of rotation of the nip roller is fixed only in the horizontal degree of freedom and is free to move vertically as well as rotate about its axis, as Fig. 1c shows. This facilitates the application of nip load vertically. In the third step, winding of the roll is accomplished by prescribing an angular velocity to the rigid core after release of the rotational constraint, as Fig. 1d shows.

For the case of center winding without a nip roller, the nip roller shown in Fig. 1 is not included in the model. At the start of these simulations, the web tension is applied in the first time step. In the second time step, the angular velocity of the core is brought to a set value.

Table I summarizes the model properties. The web thickness was intentionally set high to emphasize the ability of this modeling method to capture what will be shown to be significant bending strains and stresses in the web as part of the total stresses.

Element behavior and material constitutive laws

For the examples that will be shown, the winding problem is analyzed in plane stress conditions. Depending on the width of the winding roll, the conditions can approach plane strain, but later the results will be compared to a published winding model that was derived for plane stress conditions. The core and the nip roller were modeled as rigid analytical surfaces in these examples. The web was modeled using elastic solid four-noded isoparametric quadrilateral elements in a reduced integration mode instead of full integration mode due to computational advantages [8]. A single four-node quadrilateral element is insufficient for modeling the bending of a web through its thickness; thus, multiple elements are required through the thickness of the web. After studying various numbers of elements through the web thickness, it was concluded that four layers of elements were sufficient to model the bending effects seen by the web in the analyses conducted. In total, the winding model consisted of 10036 nodes, which defined 8026 elements and 20073 degrees of freedom.

Most materials in web form are anisotropic due to the directional orientation imparted during the forming processes. In addition, the radial modulus property, which is measured as the modulus of a web stack, is a nonlinear parameter and varies with pressure. To reduce computational time, the web is modeled as a linear isotropic material, and the stresses and strains are assumed to follow the constitutive relationship in plane stress as expressed in Eq. (1).

$$\begin{Bmatrix} \varepsilon_r \\ \varepsilon_\theta \\ \gamma_{r\theta} \end{Bmatrix} = \frac{1}{E} \begin{bmatrix} 1 & -\nu & 0 \\ -\nu & 1 & 0 \\ 0 & 0 & 2(1+\nu) \end{bmatrix} \begin{Bmatrix} \sigma_r \\ \sigma_\theta \\ \tau_{r\theta} \end{Bmatrix} \tag{1}$$

It should be noted that the commercial FE codes are capable of modeling materials with state dependent properties, but the computational expense is quite high, as the properties are evaluated in user written subroutines that may be addressed several times in a solution time step.

Surface interaction behavior

As winding begins, the bottom surface of the incoming web layer contacts the rigid core. After one revolution of the core, the bottom surface of the incoming web layer contacts the top surface of the winding roll. In the case of winding with an undriven/driven nip roller, the top surface of the incoming web layer contacts the rigid nip surface. One of the challenges in modeling a winding process using an explicit FE method is to accurately model these surface interactions. This is accomplished by modeling the contact pairs using a kinematic predictor-corrector contact algorithm [9] to strictly enforce the contact constraints that allow no nodal penetrations. The friction between all contacting surfaces is modeled using the Coulomb's friction law with a constant coefficient of friction. The Coulomb friction model relates the maximum allowable frictional (shear) stress across an interface to the contact pressure between the contacting bodies. In the basic form of the Coulomb friction model, two contacting surfaces can react

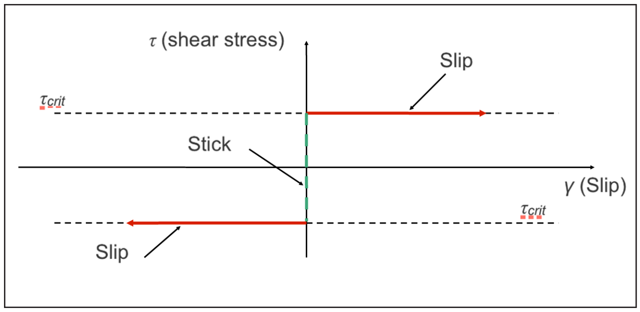

2. Schematic representation of a Coulomb friction model.

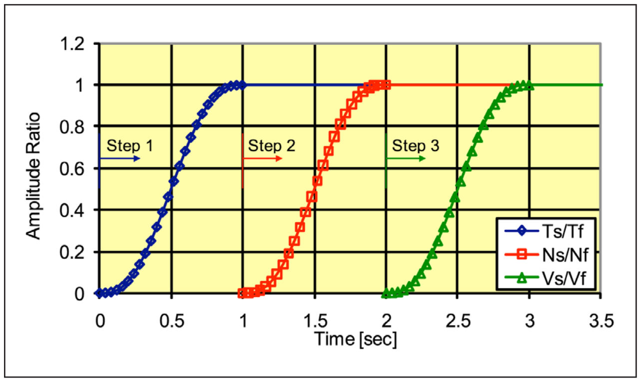

3. Behavior of web tension, nip load, and core surface velocities as a function of individual step times.

shear stresses up to a certain magnitude across their interface prior to slipping relative to one another in a state that is known as stick. This is schematically represented in **Fig. 2**.

The Coulomb friction model defines this critical shear stress (τ_{crit}) as the stress at which sliding of the surfaces starts as a fraction of the contact pressure ($p(x)$) between the surfaces, as given in Eq. (2). The stick/slip calculations determine when a point in a contact region moves from stick to slip or from slip to stick.

$$\tau_{crit} = \mu\, p(x) \tag{2}$$

The coefficient of friction (μ) in this expression can vary depending on where slippage is occurring. There can be slippage between the web and core (μ_{cw}), between web layers (μ_{ww}), and between the outer layer and the nip roller (μ_{nw}).

Loading rates and damping

For accuracy and efficiency, explicit analysis requires the application of loading that is as smooth as possible to ensure that the accelerations are low. If the acceleration is smooth, it follows that the changes in velocity and displacement are also smooth. In order to reduce the oscillatory behavior of these parameters, the amplitudes ($A(t)$) of velocity and load boundary conditions are ramped from their initial (A_s) values at time t_s to final values (A_f) at time t_f smoothly and are calculated using Eq. (3) [10]. **Figure 3** shows the different boundary conditions in the model as a function of time. It should be noted that these functions are very similar to the S curves that control engineers use to make smooth transfers from one variable state to another in web lines where the intent is also to reduce or prevent oscillatory behavior.

$$A(t) = A_s + (A_f - A_s)\xi(t)^3 (10 - 15\xi(t) + 6\xi(t)^2) \; ; \; \xi(t) = \frac{t - t_s}{t_f - t_s} \quad (3)$$

Each input parameter may induce numerical oscillation, but combinations of these inputs are even more apt to produce oscillation. Thus, each input is ramped to a final value sequentially, as Fig. 3 shows. At 1 s into the simulation, the web tension has stabilized and nip load is just beginning to increase. At 2 s into the simulation, the nip load has stabilized and velocity is just beginning to increase. At 3 s into the simulation, all input parameters have stabilized and all input conditions are steady state thereafter until the completion of the winding.

Internal damping will also limit oscillatory behavior. Damping is used for two reasons in dynamic analyses. The first reason is to limit the numerical oscillations in the solution of the systems of equations, and the second reason is to introduce physical damping when it is present and hence must be modeled. Recommended default values for damping in ABAQUS/Explicit were used in these analyses. These factors were then increased and decreased by factors of 10, and negligible impact on the results was witnessed. We concluded that the recommended default levels for damping factors were sufficient for the problem modeled.

Solution accuracy and time

The explicit procedure produces the dynamic response of the model through time in small time increments. The time increment is only conditionally stable. The stability limit is the largest time increment that can be used without generating large, rapidly growing errors in the response. An approximation to the stability limit is written as the smallest transit time of a dilatational wave across any of the elements in the mesh, as given in Eq. (4). Thus, the time increment in an explicit dynamic analysis can be very short if the mesh contains small elements (of length L_{min}), or if the stress wave speed (C_d) in the material is very high. Also, because the explicit central difference method is used to solve the equations of motion through time, the discrete mass matrix used in the equilibrium equations plays a crucial role in both computational efficiency and accuracy [11]. Mass scaling is the procedure of artificially increasing the mass of the entire or partial structure such that the smallest stable time increment can be increased to reduce the overall computational time. Per Eq. (4), the stable time increment is directly proportional to the square root of mass density (ρ). When a mass scaling factor of 'f' is used, the stable time increment increases by $\sqrt{f}$. When used appropriately, mass scaling can often improve the computational efficiency, while retaining the necessary degree of accuracy required for a particular problem [12]. It should be ensured that the changes in the mass and consequent increases in the inertial forces do not alter the solution significantly.

$$\Delta t \approx \frac{L_{min}}{C_d}; \; C_d = \sqrt{\frac{\lambda + 2\mu_L}{\rho}}; \; \lambda = \frac{E\nu}{(1+\nu)(1-2\nu)}; \; \mu_L = \frac{E}{2(1+\nu)} \quad (4)$$

In the winding FE model developed, the element length, width, mass scaling factor, and Young's modulus for the web were carefully chosen and set at 0.254 cm, 0.0635 cm, 50, and 69 MPa, respectively. A typical wound roll is made up of many layers (often thousands). However, winding an entire roll in an explicit FE code is computationally expensive. In order to study the winding problem and get a basic understanding of the development of wound roll stresses, the wound roll model was run until 13 layers were wound onto a rigid core. The analysis required an average of 60 h to complete. Desktop computers with average processing capabilities equivalent to that of an Intel Pentium IV 3.0 GHz processor with 1 MB of RAM were used for model simulations. Similar simulations on current multi-core processors will require substantially less time.

RESULTS

Wound roll stresses

Figure 4 shows the radial pressure in the wound roll as a function of wound roll length at the end of the winding process in the last time step. The radial pressure shown in the figure is calculated as the average of the centroidal stresses through the depth of each layer in the wound roll. The radial pressure in a given lap oscillates about a mean value, and the magnitude of these oscillations reduces in the laps away from the core. The radial pressure is highest at the core and zero at the outer layer as expected. The large spikes in radial pressure are produced by the upper surface of the starting edge of the web coming into contact with the lower surface of web layers in successive revolutions of the winding roll. The spikes dissipate when the wound roll builds as the bending stiffness of the web layers above the edge mutes the stress concentration of the sharp starting edge. The stress concentration of the starting edge will be discussed again later.

The tangential stress in any layer within the wound roll is comprised of both the membrane stress and the bending

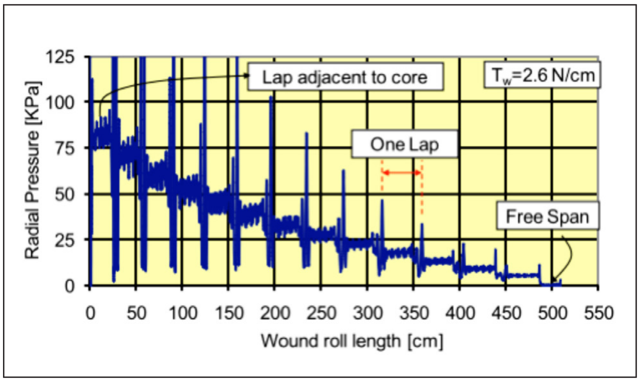

4. Radial pressure inside the wound roll.

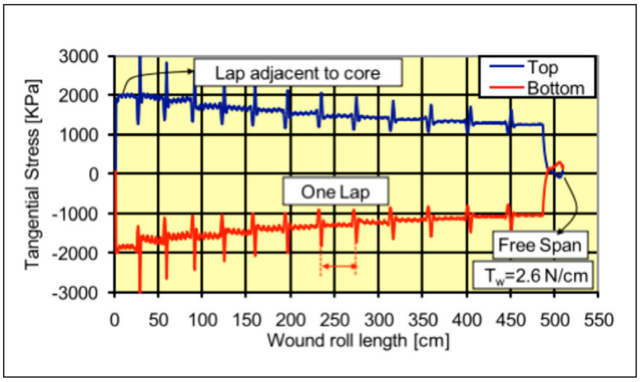

5. Total stresses in the top and bottom surface of each layer in the wound roll.

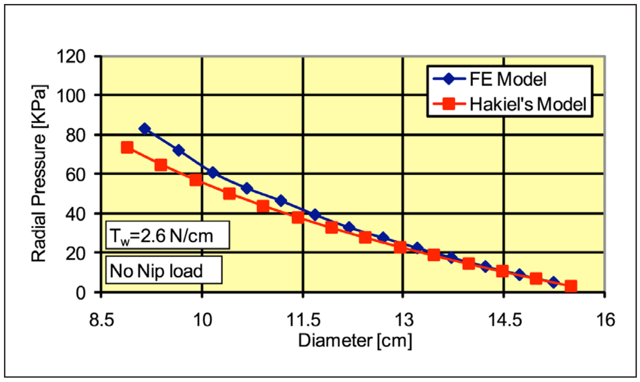

7. Comparison of radial pressure between the FE model and Hakiel's model.

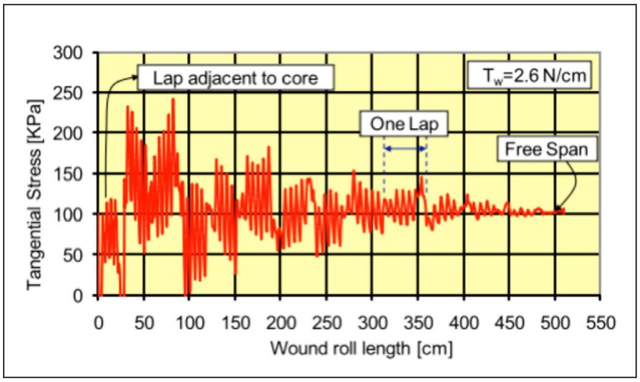

6. Tangential stresses in each lap in the wound roll.

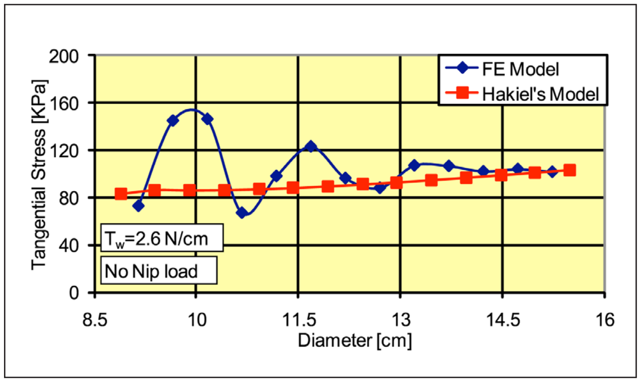

8. Comparison of tangential stresses between the FE model and Hakiel's model.

stress. **Figure 5** shows the top and the bottom surface tangential stresses in the wound roll as a function of wound roll length. The bending stresses are obviously significant in this case due to the web thickness and core diameter selected. The membrane portion of the tangential stress in a given layer can be calculated as the average of the top and bottom surface stresses and is shown in **Fig. 6**. The tangential stress behavior is noisier near the core and the magnitude of the oscillations decreases with increase in wound roll length. At the outer diameter, the tangential stress is equivalent to the stress due to web tension in the free span. Later, when winding with a nip roller, we will note the tangential stress in the outer lap is greater than that due to web tension in the free span.

Comparison with existing wound roll models

The model results for radial pressure and tangential stresses are compared to the results obtained using Hakiel's model [13] in **Fig. 7** and **Fig. 8**, respectively. Observe that the FE model results represent the average of the radial pressure and the tangential stress values in each lap taken from the data shown in Figs. 4 and 6, respectively. The radial pressure and tangential stress values from the FE model compare well with the Hakiel's model results, except near the core.

At the start of the winding process, as a new lap is laid on top of the layer adjacent to the core, the new lap encounters a radial discontinuity in the form of the web layer that is tied

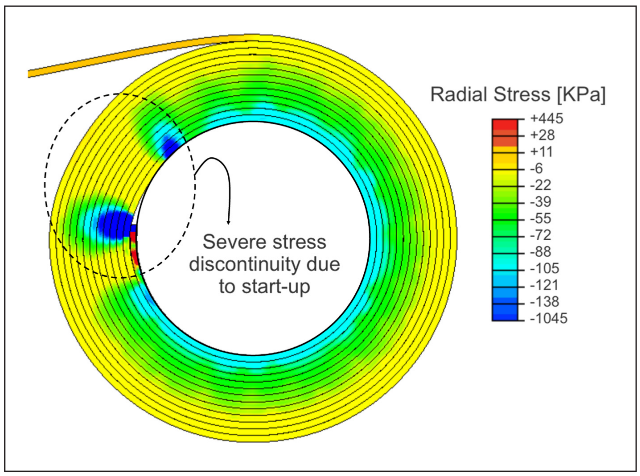

9. Stress discontinuity near the core due to web thickness.

to the core, as **Fig. 9** shows. This discontinuity (bump) creates a severe stress concentration and causes high stresses near the core. This is the reason for the disagreement between Hakiel's model and the FE model. Note that Hakiel's model incorporates an assumption that each lap in a wound roll is modeled as a concentric hoop and no discontinuities occur within the wound roll. Also, Hakiel's model is a one dimensional solution that provides the radial and tangential stresses as a function only of wound roll radius. As such, discontinui-

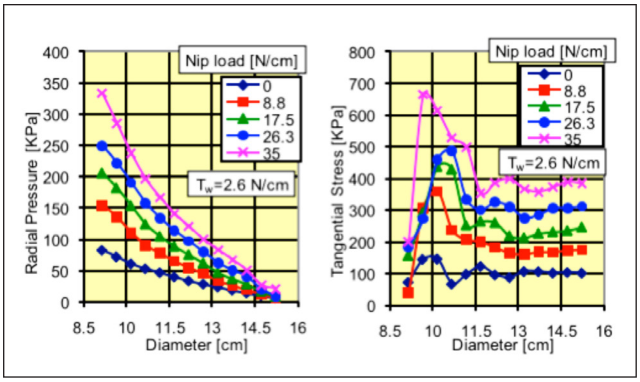

10. Effect of nip load on wound roll stresses.

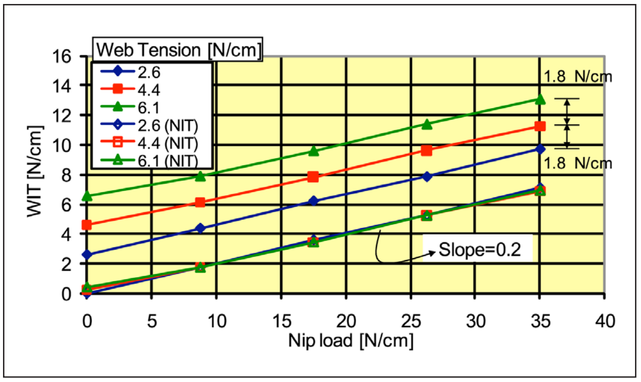

11. Effect of web tension and nip load on the wound-in-tension (WIT) and nip-induced-tension (NIT).

ties in a circumferential direction cannot be explored with one dimensional models like Hakiel's, even though these discontinuities exist in reality. As the roll grows, the stress concentration decreases, the wound roll becomes more cylindrical, and, hence, the radial pressure values compare well between the FE model and Hakiel's model. Models such as Hakiel's one dimensional winding model were never intended to account for web bending stresses. The web modeled is comparatively thick and the bending stresses are 10 to 20 times greater than the uniform winding stress in the web of 102 KPa, as Fig. 5 shows. Thus, under these circumstances, comparison of the FE results with the previous winding model results are quite good.

Effects of nip load on wound-in-tension

Figure 10 shows the effect of nip load on wound roll pressures and tangential stresses in a center wound roll with an undriven nip roller at a constant web tension of 2.63 N/cm. Although the results are not shown here, increasing the web tension increases the wound roll stresses and results in a similar qualitative behavior as shown in Fig. 10. Similar observations have been made by Good and Fikes [14]. The web tension and the nip load control the tangential stresses in the outermost layer, which in turn controls the stresses inside the wound roll. The tension in the outermost layer of a winding roll is commonly referred to as the wound-in-tension (WIT).

The portion of the WIT due to nip load is known as the nip-induced-tension (NIT). The existence of NIT was documented in tests conducted by Pfeiffer [15,16] and by Rand and Ericsson [17]. The source of the NIT involves the contact mechanics of the outer layers of the winding roll with the nip. Jorkama [18] modeled the behavior with computations. There is a finite width of contact between the surface of the wound roll and the nip due to the elasticity of the surfaces and the nip load level. As the outer layer passes through this contact zone, the normal pressure increases from zero to a maximum level and then returns to near zero pressure. Slippage will occur at some levels on the outer and inner surfaces of the outer layer, depending on web and nip elastic and friction properties. The forces of slippage combined with the web tension sum to produce the WIT.

The explicit finite element method computes the pressures of contact and the slippage forces in the nip contact zone. It also will maintain the outer layer in equilibrium, and, hence, the web tension and the forces of slippage must be balanced by the WIT. In these analyses, the WIT is expressed in terms of force per unit width of web with units of N/cm. It is calculated by multiplying the average tangential stress in the outermost layer and the thickness of the layer.

Figure 11 shows the effect of web tension and nip load on the WIT. In this case, observe that the WIT varies linearly with both the web tension and the nip load. As the web tension increases, the WIT values at different nip loads are linearly displaced by the amount of increase in web tension. The NIT is the component of the WIT that is caused due to the nip load and is calculated by subtracting the value of web tension from the WIT in a center winding process with an undriven nip. The figure indicates that the NIT is independent of web tension in a center winding process with an undriven nip roller. When the slope of the NIT curve is calculated, a value of 0.2 is obtained, and this value is equivalent to the coefficient of friction between the web layers that is given as an input to the model. This is similar to the observations of Good et al. [19]. They also observed that the WIT reduces from the maximum possible value of 'μN' at high values of nip load. This behavior is not seen in the model and is attributed to the assumptions of linear isotropic material properties for the web material.

CONCLUSIONS

The results show that modeling complex winding behaviors is possible using the explicit FE method. Now that methods exist for analysis, we can study various strategies for adhering webs to cores and core stiffness selections that will help mitigate the stress concentration associated with the start of the web on the core. We also saw the potential for large bending stresses and strains in the wound roll that, when combined with the viscoelasticity of webs, could result in machine direction curl defects. The method was also shown capable of modeling nip induced slippage and tension effects. In short, we have shown the potential for exploring many types of defects in wound rolls that were previously not possible, and the potential possibilities are exciting. **TJ**

ACKNOWLEDGEMENTS
The authors are grateful to the sponsors of the Web Handling Research Center at Oklahoma State University in Stillwater, OK, USA, for their generosity in funding this research.

LITERATURE CITED

1. Good, J.K. and Roisum, D.R., *Winding: Machines, Mechanics and Measurements*, TAPPI PRESS and DEStech Publications, Atlanta, GA, USA, 2008, pp. 157-172.
2. Hoffecker, P. and Good, J.K, *8th Int. Conf. Web Handling, Proc.*, Web Handling Research Center, Oklahoma State University, Stillwater, OK, USA, 2005, p. 565.
3. Lee, Y.M. and Wickert, J.A., *J. Appl. Mech.* 69(2): 130(2002).
4. Smolinski, P., et al., *Finite Elem. Anal. Des.* 38(6): 521(2002).
5. Li, S. and Cao, J., *J. Eng. Mater. Technol.* 126(3): 303(2004).
6. Arola, K. and von Hertzen, R., *Int. J. Mech. Sci.* 47(1): 110(2005).
7. Arola, K. and von Hertzen, R., *Finite Elem. Anal. Des.* 42(6): 503(2006).
8. Flanagan, D.P. and Belytschko, T., *Int. J. Numer. Methods Eng.* 17(5): 679(1981).
9. Dassault Systems Simulia Corp., *ABAQUS Analysis User's Manual*, Interactions, Version 6.10, 2010.
10. Dassault Systems Simulia Corp., *ABAQUS Theory Manual*, Loading and Constraints, Version 6.10, 2010.
11. Belytschko, T., Liu, W.K., and Moran, B., *Nonlinear Finite Elements for Continua and Structures*, John Wiley & Sons, Chichester, UK, 2000, pp. 310-312.
12. Belytschko, T., Chung, W.J., and Cho, J.W., *Eng. Computations* 15(6): 750(1998).
13. Hakiel, Z., *Tappi J.* 70(5): 113(1987).
14. Good, J.K. and Fikes, M.W.R., *Tappi J.* 74(6): 101(1991).
15. Pfeiffer, J.D., *Tappi* 51(8): 77A(1968).
16. Pfeiffer, J.D., T*appi* 60(2): 115(1977).
17. Rand, T. and Ericsson, L.G., *Tappi* 56(6): 153(1973).
18. Jorkama, M. and von Hertzen, R., *J. Pulp Pap. Sci.* 28(8): 280(2002).
19. Good, J.K., Hartwig, J., and Markum, R., *5th Int. Conf. Web Handling, Proc.*, Web Handling Research Center, Stillwater, OK, 1999, p. 87.

ABOUT THE AUTHORS

Web losses associated with winding are very high, and winding research has been a major focus at the Web Handling Research Center at Oklahoma State University since 1988. Many winding models have been developed in the past that have helped prevent several types of winding defects. Often, assumptions are made in the development of models that can prevent them from diagnosing all the defects we witness in the production environment. The research presented here stands out from previous work in that, for the first time, the nip-induced-tension problem was modeled in its entirety, the bending stresses that result from winding webs into rolls were modeled, and the impact of the web start at the core on local roll stresses was shown.

In this research effort, we show how explicit finite element (FE) modeling can be used to model the winding of rolls while enforcing no limiting assumptions. We show results where the effect of a web start at the core locally influences wound roll stresses and where bending stresses become part of the winding stresses. We show how nip contact influences the winding tension stress in the outer layer of the roll. These stresses can be used to diagnose contact defects due to the web start and due to nip contact, curl defects due to bending, and bursts due to nip induced slippage.

The most difficult aspect of the explicit FE modeling used in this research involved the solution of very large sets of equations of motion, which can require many days of computation to solve. We addressed this aspect by carefully choosing the elements and mesh density for the problems modeled.

Kandadai

Mills can benefit from this information by knowing that there are new modeling methods available to help them explore a greater range of roll defects, and that these models can be used to determine winder operating conditions that prevent defects. Our future research will include the study of other wound roll defects using this method, as well as to encourage use of this modeling method for winding rolls and exploring ways to improve roll quality.

Good

Kandadai is a research assistant and Good is professor at Oklahoma State University in Stillwater, OK, USA. Email Good at james.k.good@okstate.edu.